THE PERMEABILITY OF SILICA AEROGELS

Thierry Woignier, Liz Anez, Sylvie Calas-Etienne, Juan Primera, Pascal Etienne, Jean Phalippou

THE PERMEABILITY OF SILICA AEROGELS

Thierry WOIGNIER (1,2), Liz ANEZ (3), Sylvie CALAS- ETIENNE (4),
Juan PRIMERA (5), Pascal ETIENNE (4), Jean PHALIPPOU (4)

[1] Aix Marseille University, University Avignon, CNRS, IRD, IMBE, Marseille, 13397, France
[2]Institut Méditerranéen de Biodiversité et d'Ecologie, Campus Agro Environnemental Caraïbes, B.P. 214 Petit Morne, 97232 Le Lamentin, France
[3] Departamento de física, Universidad del Zulia, Maracaibo, Venezuela
[4]Laboratoire Charles Coulomb (L2C), Université Montpellier, 34095 Montpellier, France
[5] Universidad Técnica de Manabí. Instituto de Ciencias Básicas. Departamento de Física., Avenida Urbina y Che Guevara. Portoviejo Provincia de Manabí, República del Ecuador

Corresponding author: Thierry Woignier: thierry.woignier@imbe.fr

Keyword(s)
Gas and liquid *permeability,* aerogels, sintered aerogels, composites aerogels*, Klinkenberg* factor, Knudsen correction, fractal microstructure.

Abstract

Silica aerogels have many potential applications, including as host matrices for chemical species or nuclear waste storage. For these applications, the *permeability* is a key parameter and data show that the silica aerogels have poor *permeability* (~10-60 nm^2). In this chapter we review the method to measure the liquid and gas permeability in gels, aerogels and composite aerogels. Ideally, *permeability* does not depend on the type of pore fluid, therefore *permeability* measured using gas should be the same as that measured using water. We measured gas and water *permeability* in sets of nano composite silica aerogels. Experimental results show that gas *permeability* in aerogels was larger than water *permeability* by almost two orders of magnitude. The observed difference in gas and water *permeability* was analyzed from the point of view of the slip regime (*Klinkenberg* correction), and transition regime (Knudsen correction), the slip flow of gas at pore walls enhance the gas flow when pore sizes are small. This work addresses the problem of estimating *permeability* with high porosity materials such as aerogels. The effects of structural parameters of porous media (pore volume, tortuosity, fractal features) on the *Klinkenberg* and *Knudsen* corrections are discussed and the different models proposed in the literature are tested.

1) Introduction

Aerogels have been attracting increasing interest in diverse domains ranging from fundamental research in physics to their application as specific materials. Silica aerogels have many potential applications, including as catalyst supports, insulators, acoustic materials, and space applications, and the number of potential uses of aerogels is even higher if it is considered not only as an end product but also as a precursor, for example, as a host matrix for chemical species (drugs, nuclear waste storage, etc.). Silica aerogel concerns the synthesis of multi-phase materials, doped material, multi-component glasses, and composites [1]. In this case, the large pore volume is used as a sponge to incorporate chemical species to obtain a two-phase material. The chemical species are first processed in liquid form, but aerogels tend to crack during filling because of capillary forces [2]. In this process, *permeability* is the most important parameter.

In fluid mechanics, permeability is a measure of the ability of a porous material to allow fluids to pass through it. The *permeability* is related to the porosity, but also to the shapes of the pores in the medium and their level of connectivity.

Generally, high *permeability* is an advantage because it means the fluid and hence the chemical species of interest migrate easily in the porous network and homogeneous distribution of the chemical species can thus be expected. Unfortunately gels and aerogels usually have low *permeability ,* only a few nm^2 [3-8].

The low *permeability* of silica gels is also the main property responsible for gel cracking during the different steps of the different drying process (evaporation, heating and depressurization).

In the standard drying process, the gel shrinks until the liquid at the network surface enters the pores. The evaporation rate of the liquid depends on the rate of *permeability* of the gel. As a result, in the case of rapid evaporation rates and low gel *permeability* , the pressure (or stress) gradient between the liquid located at the surface and that in the sample core is high enough to cause cracking [3,9].

Supercritical drying (SCD) usually enables the preparation of large monolithic gels by eliminating the capillary stresses that cause damage during evaporation in ambient conditions. Nevertheless, cracking sometimes occurs during supercritical drying, mainly linked to the mechanical properties of the samples, but also to low *permeability* . The first step of supercritical drying consists of heating the gel in an autoclave. During heating, expansion is expected and the gel is under tensile stress. If the samples are too large and the heating rate too fast, cracking will occur [10,11].

Cracks can also appear during the depressurization step [12,13]. When the pressure and the temperature are higher than the temperature corresponding to the critical point of the solvent, a valve is opened to depressurize the autoclave and transform supercritical fluid into gas. If the valve is opened too fast, the pressure of the superfluid inside the gel remains higher than that of the superfluid surrounding the sample. Because of the low *permeability* of the gel, the pressure outside the gel will drop faster than inside. This pressure gradient can cause the gel to crack [13]. For these different process and applications, *permeability* is thus a key parameter.

The physics of flow through porous media [14] has received considerable attention due to applications including petroleum engineering, water purification, and soil mechanics. In the energy sector, there has been a significant increase in the production of gas from shale strata. Due to the importance of these low *permeability* reservoirs in gas production, extensive research has been conducted on these types of resource and models developed [15]. Because of their peculiar structure and low *permeability* , aerogels are useful porous structures to test models that extrapolate permeability from structural parameters.

In this chapter, we review the methods used to measure *permeability* (liquid and gas) in silica gels and aerogels. Ideally, *permeability* does not depend on the type of pore fluid; therefore, permeability measured using gas should be the same as that measured using water. However, experiments have shown that gas *permeability* in gels can be one order of magnitude greater than water permeability [16]. The observed difference in gas and water *permeability* has been analyzed from the point of view of the *Klinkenberg* or *Knudsen* corrections [17,18].

This chapter addresses the problem of estimating *permeability* with high porosity and very brittle materials such as aerogels.

2) Experimental techniques to measure the *permeability* of gels and aerogels

The *permeability* (D) of a porous material is a property that accounts for the ability of a fluid to flow through the porous network and is expressed by Darcy's law:

$$J = - D/\eta \nabla P \qquad (1)$$

The flux (J in $m.s^{-1}$) is inversely proportional to the viscosity η (Pa.s) of the liquid. The flux also depends on the pressure gradient (∇P) applied to the liquid. *Permeability* has the dimension of a surface and is expressed in unit $length^2$.The usual way to measure the *permeability* of a

porous material is to estimate the amount of liquid that goes through it per unit of time. However, because of the small pore sizes of gels, the flux of liquid is generally difficult to measure. Alternative methods (relaxation methods), based on the difficulty liquid has flowing in the porous structure, have been proposed in the literature to measure the *permeability* of the gel and aerogel.

2a) Relaxation methods

2a1) Thermal expansion method

The *permeability* of the gel can be deduced from the thermal expansion method [19]. This method takes advantage of the low mechanical properties of gels. In summary, the gel containing a non-reactive liquid such as an alcohol is rapidly heated. During the heating run (Q in the figure) , the liquid within the pores has no time to escape from the solid network (Figure 1). Because of the low elastic properties of the network, the net result is the expansion of the solid.

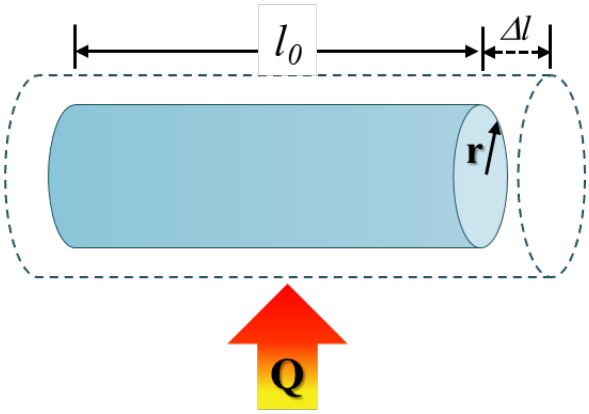

Figure 1. Schematic representation of thermal expansion experiments designed to measure D (Q is the heating run) .

If the gel is then maintained at constant temperature, the liquid progressively leaves the pores. The sample contracts to its initial dimension. Some authors (19) have shown that the experimental curve can be fitted with a theoretical equation containing a hydraulic relaxation time (t). This relaxation time contains parameters related to the liquid and the solid phases, respectively.

$$D = \eta\, r^2/Ht, \qquad (2)$$

where (r) is the radius of the cylindrical sample, η (Pa.s) is the viscosity of the liquid and H (Pa) is the elastic longitudinal modulus of the sample.

2a2) Three-point bending

Another way to measure the *permeability* is the three-point bending method performed in a liquid [11]. A sample is suddenly deformed at a selected strain rate (Figure 2). In the first instant, the liquid cannot escape from the gel, the sample deforms but its whole volume remains constant. Thus, the sample behaves as an incompressible fluid with a *Poisson* coefficient (υ) equal to 0.5 and an apparent *Young's modulus* (E_a in Pa):

$$E_a = 2G(1+\upsilon)=3G \qquad (3)$$

G (Pa) is the shear modulus. With time, the liquid is able to leave the pore network, the *Poisson* coefficient is now 0.2, and the real *Young's modulus* is then obtained. As the pore pressure equilibrates, the force required to sustain a constant deflection decreases; *permeability* can be obtained by fitting the force decay to the theoretical expression [20,21]. The curve W(t)/W(0) (where W is the applied force) is followed and the rate of load relaxation is used to calculate the permeability :

$$D = \eta\, l^2(1-2\upsilon)/Gt, \qquad (4)$$

where η is the viscosity of the liquid, 2l is the edge length of the sample squared cross section and t is the relaxation time.

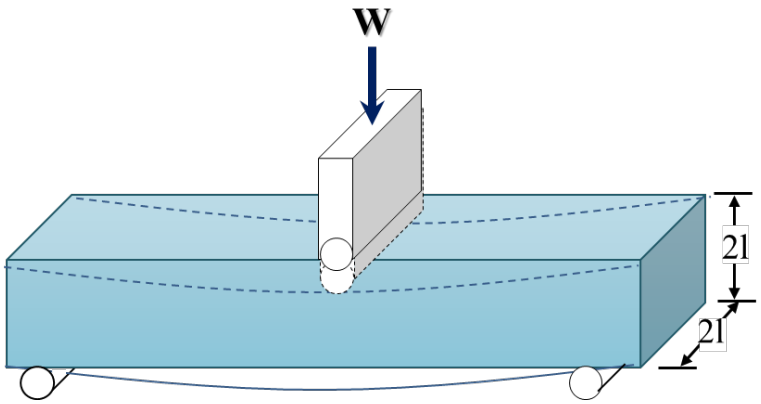

Figure 2 Schematic representation of 3-points bending experiments designed to measure D .

In the literature [8,11-13,19-22], these different methods have been successfully applied to silica alcogels. Results showed that the *permeability* of gels depends on their nature. For acid-catalyzed gels, *permeability* is in the range of 1-5 nm^2, 5 -10 nm^2 for the neutral alcogel and 10-20 nm^2 for base-catalyzed samples and two-step processes. These values confirm the low *permeability* of silica gels and the influence of the gelling conditions on network permeability .

Scherer [20] also studies the effect of a classical drying on the alcogels (two steps–process) *permeability* . He shows that the *permeability* decreases by almost four orders of magnitude as the gels contracts (the relative density increases from 0.073 to 0.457)

2a3) Impregnation method

However, these methods are based on the large compliance and the small pore size of the porous network, and are not appropriate for stiffer material and/or materials with larger pores. We thus proposed to derive the *permeability* from impregnation experiments [23,24].

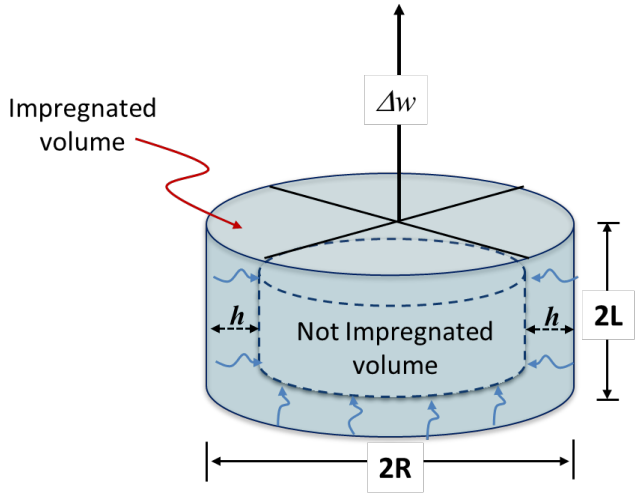

Figure 3. Schematic representation of impregnation experiments designed to measure D . Adapted from [23].

The samples are dipped in a liquid and any changes in the apparent weight are monitored. During impregnation h(t), the thickness of the penetrating liquid increases with time (figure 3). When the impregnation proceeds, as a function of h(t), the Archimedean force decreases proportionally to the filled pore volume.

Darcy's law for a small-impregnated volume is:

$$dV_{imp} / dt = D/\eta \, \Delta P.A(t)/ h(t) \qquad (5)$$

where D is the *permeability* , A(t) the normal surface of the flow, η the liquid viscosity, and $\Delta P/h(t)$ the pressure gradient in the liquid. Considering h(0) = 0, we find

$$h^2(t) = 2D \, \Delta Pt/\eta\phi \qquad (6)$$

where ϕ is porosity; h(t) can be expressed as a function of V_{imp}/V_p and derived from the Archimedean force experiments [23].

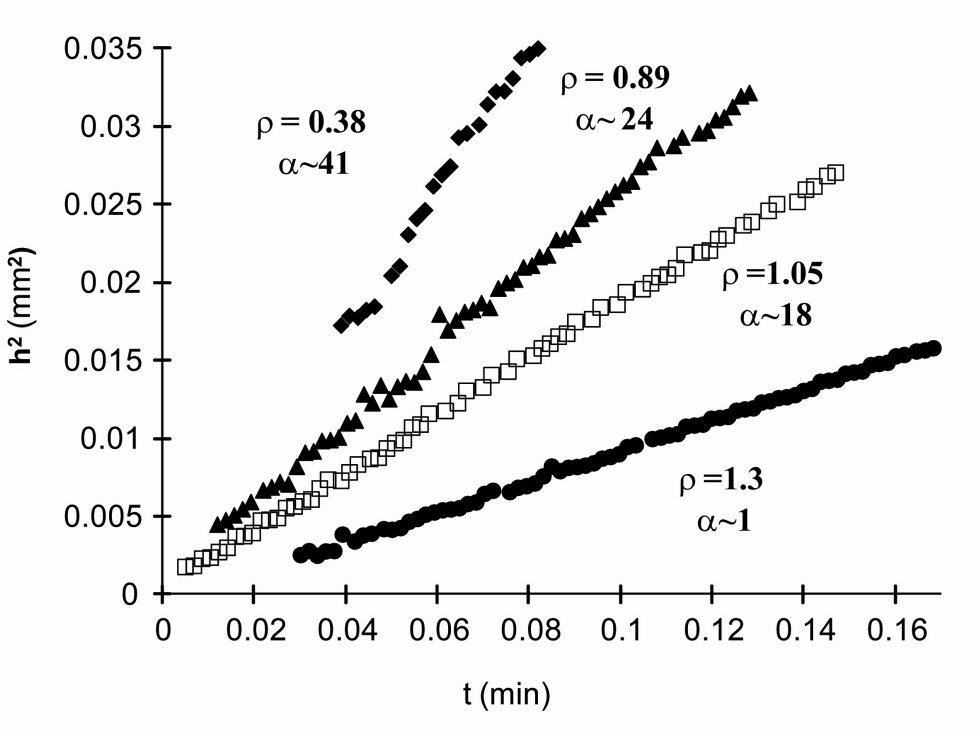

Figure 4: Impregnation curves $h^2(t)$ versus t for silica aerogels with various bulk densities. Adapted from [23]

Thus, by plotting $h^2(t) = f(t)$, it is possible to calculate the slope α and D is equal to:

$$D = \alpha\phi r_h \, \eta/(4\gamma\cos\theta) \qquad (7)$$

where ϕ is porosity, r_h is the hydraulic radius and θ is the wetting angle. Capillary forces are the driving forces for fluid migration and ΔP is the capillary pressure. Our experimental results have shown that the curves $h^2(t) = f(t)$ are in agreement with the expected linear behavior and that

using η (0.355 10^{-3} Pa.s) and γ is the interfacial energy (0.0725 J m^{-2}) for water, it is possible to calculate D [23]. Figure 4 shows the impregnation curves $h^2(t)$ versus t measured on sintered aerogels with bulk densities ranging from 0.39 to 1.3g.cm^{-3}

2a4) Gas *permeability*

The experimental technique (figure 5) used to measure the gas *permeability* D_{gas} was based on Darcy's expression for the description of one-dimensional homogenous flow through porous media when compressible gas is used as pore fluid [14, 16]:

$$D_{gas} = (dV/dt)\ (L\mu/A)\ (2P_b)/(P_1^2-P_2^2) \qquad (8)$$

where dV/dt is the flow rate or volume variation (dV) per time unit (dt), μ is the gas viscosity (Pas) , A is the sample cross-sectional area to flow, L is the sample length, P_1 and P_2 are sample intake and exhaust pressure (Pa), and P_b is the atmospheric pressure (Pa). Measurements were made with N_2 and the experimental setup allowed D_{gas} measurements over mean pressures ranging from 500-1000 hPa. The experimental data are given for a mean pressure of 900 hPa. Details on the techniques can be found in references [16]. A previous study showed that D_{gas} ranged from 80 to 175 nm² for composite xerogels [16].

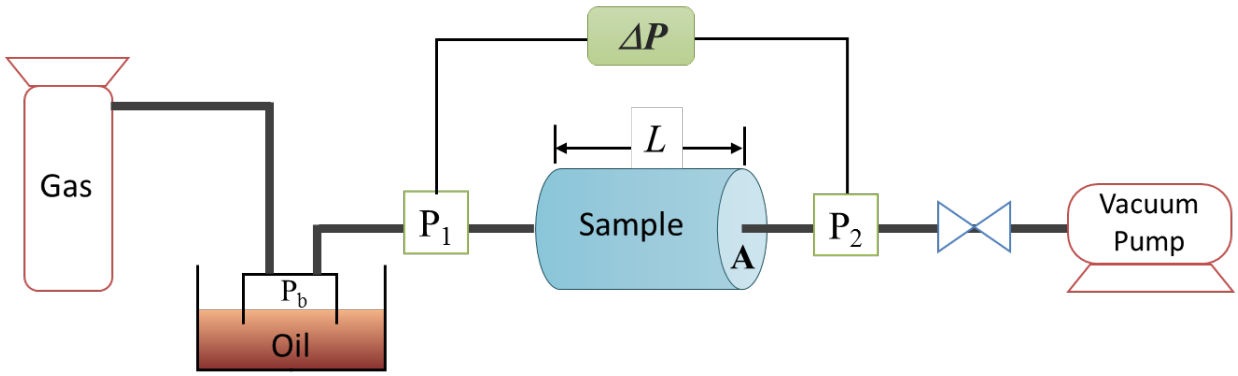

Figure 5. Schematic representation of gas flow experiments designed to measure D .

2a5) Empirical relation

In the literature, the *permeability* of porous material is sometimes calculated from empirical relations using the textural properties (mean pore radius, density, specific surface area).

$$D = (1- \rho_r)^3 / \ K (\rho_r S \rho_s) \quad (9)$$

where ρ_r is the relative density, S is the specific surface area ($m^2.g^{-1}$) and ρ_s is the skeletal density ($\approx$ 2 $g.cm^{-3}$) [2, 9]. The Carman Kozeny relation [25] is usually used for porous materials for which an empirical constant (K) close to 5 is accepted [9]:

However, Primera et al. [26] showed that for some silica xerogels and aerogels, the K value can vary between 1.7 and 17, which clearly differ from a value of 5.

Scherer proposed an expression of the Carman Kozeny equation that relates the *permeability* to the pore size of gels [22]:

$$D = (1 - \rho_r) r_w^{\ 2} / 4K_w \quad (10)$$

where ρ_r is the relative density, r_w is the characteristic pore size that governs *permeability* [27], and K_w is the so-called Kozeny constant. However, in the case of gels (broad pore size distribution) Scherer explains that r_w is close to the hydraulic radius. Moreover, K_w is not constant but a function of ρ_r [20]. Over the range of density used in the Scherer study [28], it can be approximated by:

$$K_w = 2.03 + 2.56\rho_r, \quad 0.08 \le \rho_r \le 0.4. \quad (11)$$

Thus, from the relative density and the hydraulic radius, it is possible to estimate the *permeability* of the aerogels.

Another empirical approach is proposed in [28] on partially dried silica gel by aging, a power law dependence on density:

$$D = D_0 (\rho/\rho_0)^{-n} \quad (12)$$

where D_0 and ρ_0 are, respectively, the permeability and the density of the sample before aging. For the samples Scherer studied n was found to be $\approx$2.46 [28].

3) Results

3a) Relaxation methods with aerogels

The *permeability* measured by thermal expansion and three-point bending for silica alcogels is usually in the range of 0.06-20 nm^2 [12,20]. In the case of aerogels, it is difficult to measure the *permeability* by thermal expansion, three points bending or impregnation techniques based on the behavior of a liquid inside the porosity. It would be necessary to refill the porosity with a liquid but generally, the dried aerogel cracks during the filling. To solve this problem, *permeability* can be measured on a "re-wetted" aerogel [13,22]. With these samples, the supercritical heat treatment is not followed by evacuation of the superfluid, so the solvent invades the gel during cooling. This procedure allows to prepare materials, full of solvent, for which the solid network has undergone the same heat treatment as for classical aerogels and consequently the same structural changes, associated with the supercritical drying.

Sample	Permeability (nm^2)	Sample	Permeability (nm^2)
Neutral alcogel	2.9	Base alcogel	8.5
Neutral rewetted aerogel	3.9	Base rewetted aerogel	9.8

Table 1: *Permeability* of base and neutral silica alcogels and rewetted aerogels

The results showed a small increase in permeability after supercritical drying [13]. Regardless of the catalyst used, the re-wetted aerogel *permeability* was low, in the range 3–10 nm^2 (table 1).

3b) Impregnation methods

3b1) Sintered aerogels

The impregnation method was successfully applied on aerogels strong enough to resist capillary stresses during the liquid impregnation step. Thermal treatments allow the aerogels to be converted into porous glasses and the final density of the sintered aerogels will depend on the thermal treatments applied [2]. In the temperature range 1050–1075 °C, the pore volume is

completely collapsed and the bulk density is close to 2.2 g.cm^{-3} i.e. the silica glass density. Experiments performed at 800 and 950 °C, as a function of time, allow a precise control of the density by sintering. It is thus possible to synthesize partially sintered aerogels in the density range 0.25–1.4 g·cm^{-3}.

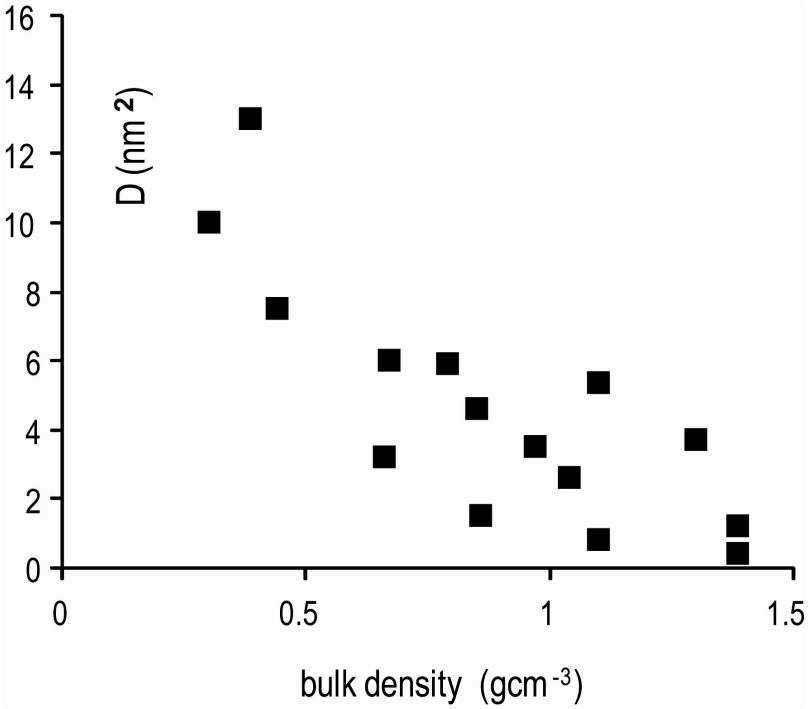

Figure 6: Changes in D versus the silica aerogel bulk density

For example, figure 6 shows changes in *permeability* as a function of the bulk density for partially sintered silica aerogels [1,2]. This figure clearly shows that D decreases considerably with sintering. As explained above, sintering proceeds first by collapsing the smallest pores, then at high density, the mean pore size becomes so small that *permeability* tends to 0. These results are qualitatively in agreement with the empirical Carman-Kozeny relation (see 2a5). According to this relation, because of the decrease in the mean pore size and the increase in relative density, D decreases. So a compromise in density needs to be found for the use of sintered aerogels as host matrices. Bulk density has to be high enough to obtain a matrix with acceptable mechanical properties but not too high, to have significant *permeability* and pore size. This compromise corresponds to a bulk density in the range 0.8–1 g cm^{-3} [2].

3b2) Composite aerogels

Composite aerogels are synthesized by adding silica particles (pyrogenic silica aerosil OX 200 DEGUSSA) in the gelling solution. Details on the synthesis are given in references [1, 16, 29]. First, a wet composite gel was obtained by hydrolysis and polycondensation reactions of organosilicate compounds (tetraethylorthosilicate, TEOS) dissolved in ethanol. TEOS was hydrolyzed with 15 moles of water (HCL 10^{-2}M) per mole of TEOS under stirring for 1 hour to favor hydrolysis. Pyrogenic silica was added under stirring and the pH was adjusted to 4.5, leading to gelation in a few minutes. The weight of the pyrogenic silica as a percentage of the total silica weight, ranged between 0% and 55%.

To consolidate the gel structure, the samples were aged for seven days at room temperature. The nanocomposite wet gels were then transformed into aerogels by supercritical drying with ethanol (305 °C, 13 MPa). The bulk density varies between 0.25 and 0.45 $g \cdot cm^{-3}$

The *permeability* of the composite aerogel set has been measured by the impregnation method [23,24] and Fig. 7 shows changes in D as a function of the *aerosil* content. These data clearly show the improvement of the *permeability* for *aerosil* content higher than 50 % despite the higher bulk density.

In contrast to sintered aerogels, the *permeability* of composite aerogels increased with an increase in the aerosil content and hence an increase in density [24] (Figure 8). This counterintuitive result (with respect to the Carman-Kozeny relation) is due to the fact that while the addition of aerosil particles increases the density, it also increases the mean pore size [24]. The net result is an increase in *D*. The composite aerogel set combines improvement of the mechanical properties, and an increase in mean pore size and hence in *permeability* . This method is easy to use, produces host matrices with a large porous volume that is accessible and can be rapidly impregnated by standard liquids such as water or ethanol. [23,24].

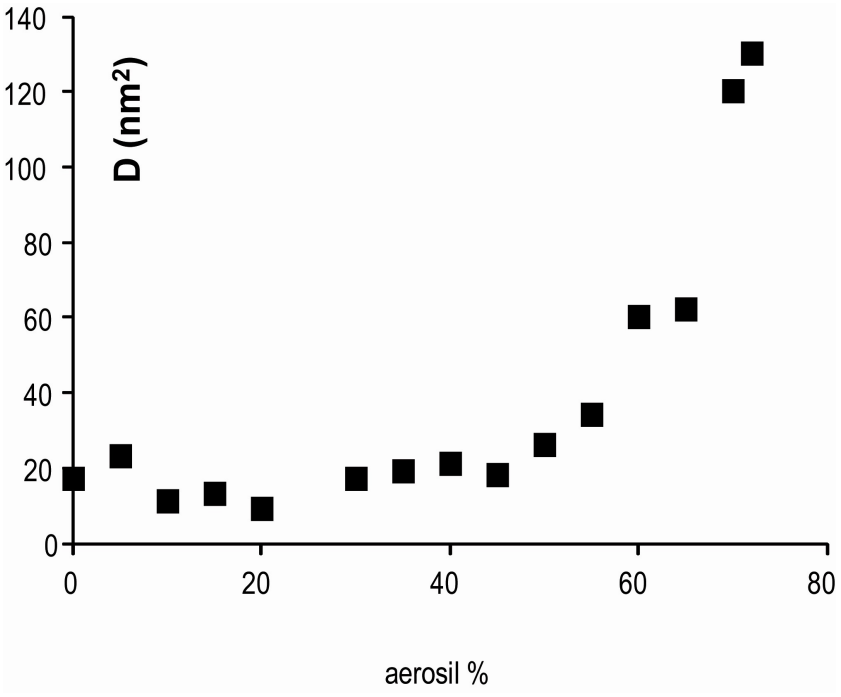

Figure 7: Liquid *permeability* of nanocomposite aerogels versus aerosil content. Adapted from [24]

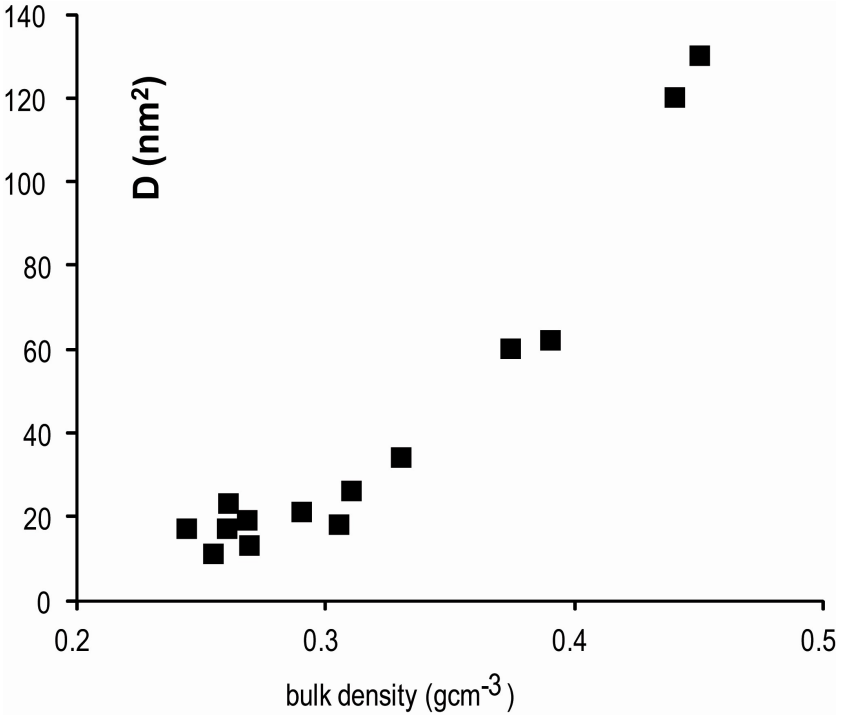

Figure 8: Liquid *permeability* of nanocomposite aerogels versus bulk density. Adapted from [50]

3c) Gas *permeability*

Another way to determine the *permeability* of an aerogel is using the gas permeability technique. Ideally, *permeability* is a property of the porous structure and does not depend on the kind of pore fluid. Intrinsic *permeability* describes the mobility of fluid within a porous material and is only related to the pore geometry of the porous material. Consequently, *permeability* measured by any gas (D_{gas}) should be same as intrinsic *permeability* measured by liquid (D). However, in pores with a diameter comparable to the mean free path of the gas molecules, the additional flux due to gas flow at the pore walls (the slip flow of gas) actually increases the gas flow rate. We will show in the following that this slippage effect increases the apparent *permeability* .

3c1) Composite aerogels

Although *permeability* should not depend on the pore fluid, experimental data on comparable gels showed that when measured with gas [4], *permeability* is systematically higher than liquid permeability [10,23]. A previous study on composite xerogels [16] showed that both liquid and gas permeability increased with an increase in aerosil content, while D ranged from 3 to 9 nm² ,D_{gas} ranged from 80 to 175 nm² for composite xerogels [16].

Aerosil content (%)	Porosity	D_{gas} (nm^2)	Hydraulic diameter (nm)
0	0.88	1095	77
5	0.87	1260	80
10	0.87	1450	96
15	0.87	1440	111
25	0.87	2090	138
35	0.87	2100	169
45	0.85	1675	132
55	0.83	2093	133

Table 2: Porosity, gas *permeability* and hydraulic diameter of composite aerogels versus aerosil content.

.

These results on aerogels confirm data in the literature. The comparison of Fig 7 and table 2 shows that D_{gas} is two orders of magnitude higher than D. Previous studies showed that, under confinement, the physical properties of fluids deviate from their bulk value [30,31]. In such tiny pores, the effects of the interaction between the pore walls and molecules become significant, and fluid properties such as critical properties, phase behavior, solubility, and viscosity change dramatically [32-35]. In microporous media, *permeability* differed with pore size and this phenomenon was attributed to gas slippage [36-38].

4) Correction factors for slip regime and transition regime.

Gas slippage is defined as the condition in which the mean free path of the gas molecules is no longer negligible compared to the average pore radius. Flow under confinement deviates from Darcy type flow, as gas molecules slip on the surface of the pores. This phenomenon causes an increase in D_{gas} [37]. The additional contribution to gas transport results from the frequent collision of gas molecules with the pore walls. The Knudsen number (Kn, the ratio of the mean free path of the gas to the pore diameter) [39], classified gas flow in four flow regimes: the continuum flow regime ($Kn < 0.001$), the slip flow regime ($0.001 < Kn < 0.1$), the transition flow regime ($0.1 < Kn < 10$) and the free molecular flow regime ($Kn > 10$). We now discuss the slip and transition flow regimes that correspond to the present materials. In slip flow, the *Klinkenber*g model [37] approximates a linear relationship between measured gas *permeability* (D_{gas}), liquid (intrinsic) *permeability* (D), reciprocal mean pressure (P_m), and the Klinkenberg factor (b):

$$D_{gas} = D\,(1+b/P_m) \qquad (13)$$

The slippage effect increases D_{gas}, but at high mean pressures, the slippage effect is suppressed and gas *permeability* is reduced until, at infinite mean pressure, the mean free path is reduced to zero. Gas is consequently considered to behave like a liquid, and gas and liquid *permeability* should be the same.

The transition regime is referred to as a flow regime where both slip and diffusion flows can occur. This is a flow regime in which the traditional fluid dynamics equations could be applied, i.e., Darcy, with Knudsen's correction:

$$D_{gas} = fc\ D \quad (14)$$

where *fc* is the Knudsen correction factor (40). At room temperature and at 900 hPa, the mean free path of N_2 is 64.9 nm. The microstructure of nanocomposite silica gels is an assembly of aggregates and pores (5-200 nm) (29) and the hydraulic diameters of the nano-composite aerogels (80-170 nm) (table 2) are in the range of the N_2 mean free path.

Aerosil weight (%)	Kn	*Klinkenberg* factor *b* (MPa)	*Knudsen* factor fc
0	0.83	5.71	72
5	0.80	10.8	71
10	0.66	10.8	135
15	0.57	9.88	124
25	0.46	11	137
35	0.38	9,86	123
45	0.48	7.09	87
55	0.48	5.45	69

Table 3 : Knudsen number (Kn), Knudsen correction factor (fc) and *Klinkenberg* factor (*b*)versus aerosil content.

In the set of samples studied, Kn ranged between 0.48 and 0.83, i.e. in the range of the transition regime and at the boundary of the slip regime. Consequently, for these materials, gas slippage in either the transition or the slip regime can be expected and we analyze the data with the *Knudsen* factor correction but also with the *Klinkenberg* approach. Figures 4 and table 2 allow us to calculate the experimental *Knudsen* correction factor (fc) and the *Klinkenberg* slip factor (b) (table 3). The correction factor *fc* is high, in the range 70-140, and the calculated *b* factor varies in the range 5–11 MPa. The resulting values decrease with an increase in the concentration of pyrogenic silica, confirming that factor *b* varies conversely to pore radius [32].

4a) *Knudsen* correction

When the Knudsen number corresponds to the transition regime, different researchers have proposed equations to calculate *fc* [40, 48,49] (see table 4). Tang et al. (48) suggested:

$$fc = (1 + A/Pm + B/Pm^2) \quad (15)$$

$$\text{where } A = C_1 (8 \mu / d_h) (\pi RT/2)^{0.5} \quad (16)$$

$$\text{and } B = C_2 (8 \pi RT (\mu / d_h)^2, \quad (17)$$

μ is the dynamic viscosity of the gas (Pa.s), and d_h is the hydraulic diameter (Table 2). C_1 and C_2 are respectively in the range 1-1.46 and -0.5- $5\pi/12$.

Florence et al [18] developed a second order equation in which *fc* depends on the *Knudsen* number:

$$fc = [1 + \alpha(Kn)\, Kn] (1 + 4Kn/1+Kn), \quad (18)$$

A correlation is provided to calculate α the rarefaction coefficient α:

$$\alpha = \alpha_0\, 1 + AKnB, \quad (19)$$

(where A = 0.170, B = 0.4348, and α_0 = 1.358);

Ziriani et al. (40) proposed the following relation:

$$fc = [1 + \alpha_0 (1 + AKnB)\, Kn] [1 + 4Kn/(1+Kn)] \quad (20)$$

However, the experimental fc values (Table 3) are very high: 70-140, i.e. 30-50 times higher than the model predictions found in the literature [18,40,48,49].

Sample	Equations transition regime (fc factors)	References
Theoretical formulation	$fc = 1 + A/Pm + B/Pm^2$	48
Data in the literature and from industrial sources	$fc = (1 + \alpha(Kn)\, Kn) (1 + 4Kn/(1+Kn))$	18
Data in the literature and from industrial sources	$fc = (1 + \alpha_0 (1 + AKnB)\, Kn) (1 + 4Kn/(1+Kn))$	40
Data in the literature and from industrial sources	$fc = (1 + 6B1\, Kn + 12B2Kn^2)$	49

Table 4: Overview of existing *Knudsen* factor correlations.

A = C1 $(8\,\mu / D_h)\ (\pi RT/2)^{0.5}$ and B = $C_2\,(8\,\pi RT\,(\mu/D_h)^2$. D_h is the hydraulic diameter, R is the gas constant, *T* is the temperature, *Pm* is the mean pressure and μ the dynamics viscosity of the gas. The coefficient C_1 and C_2 are respectively in the range 1-1.46 and 0.14 -5π/12 (48) . α is dimensionless rarefaction coefficient. $\alpha = \alpha_0\ 1 + A\ Kn\ B$, where A = 0.170, B = 0.4348, and α_0 = 1.358. (40,53).

The coefficient B1 and B2 are respectively in the range 1-1.146 and -0.5- 1 (56- 57)

4b) *Klinkenberg* approach

If we consider a *Klinkenberg* approach, some authors [41-46] proposed empirical equations to calculate *b*; they are known as *Klinkenberg*'s first order equations (see table 5):

$$b = A\,(D)^{-B} \qquad (21)$$

where A and B are empirical values that make it possible to fit the experimental data, and for different permeability ranges of between 10^{-12} and 10^{-22} m^2.

In addition to these empirical relationships, some authors used theoretical approaches (17,18,47). Florence et al. [18] developed a theoretical formula linking *b* to the ratio (D/ϕ), with an exponent equal to −0.5.

$$b = \beta\,(D/\phi)^{-0.5} \qquad (22)$$

β is a parameter that depends on the type of gas used .

Civan [17] proposed a similar expression but also using the tortuosity factor τ:

$$b = \mu(\pi RT/\tau\ Vg)^{-0.5}.\ (D/\phi)^{-0.5} \qquad (23)$$

where Vg is the gas molar volume, T is the temperature, R is the universal gas constant, and μ is viscosity (Pa.s).

The empirical equations traditionally used to estimate the b factor are far from the experimental values (10 times lower). *Permeability* estimated using the different theoretical equations that include porosity and tortuosity still differed from measured *permeability* by a factor of 5 .

More recently, Song et al [47] proposed a relationship that made it possible to calculate *b* for fractal materials:

$$b = 1.25\ (8\mu\ (3+\lambda-D_f)/(2+\lambda-D_f))(32\ \tau\ (4-D_f/(2-D_f))\ (1-\phi)^{-0.5}\ (\pi RT/(2M))^{-0.5}(D/\phi)^{-0.5} + 0.23\ (8\mu\ (3+\lambda-D_f)/(2+\lambda-D_f))(32\ \tau\ (4-D_f/(2-D_f))\ (1-\phi)^{-0.5}(\pi RT/(2M))\ (D/\phi)\ (1-(\xi_{max}/\xi_{min})^{1+\lambda-D_f}) \quad (24)$$

λ and D_f are the fractal dimensions for tortuosity and for pore space. The predictions of the Song et al model are in a quite good agreement with the experimental data [51]. So, introducing fractal features [47,51,52] clearly improves the accuracy of the prediction.

The paradox of these porous structures is that they are highly porous but poorly permeable and most of the empirical and theoretical models proposed in the literature for the transition or the slip regimes are not able to account for the marked discrepancy between experimental *permeability* when measured with gas or with liquid. Further theoretical models and investigations are needed to describes the slip and transition regimes in fractal and highly porous media like aerogels.

Sample	Equations slip regime (*Klinkenberg* factors) (Pa)	References
Sedimentary rocks	$b = 0.15\ (D)^{-0.37}$	41
Oil-field cores	$b = 0.189\ (D)^{-0.36}$	42
cores ranging	$b = 0.11\ (D)^{-0.39}$	43
tight gas sand samples	$b = (D)^{-0.33}$	44
Suite of cores from a sea gas reservoir.	$b = 0.14\ (D)^{-0.38}$	45
10 core samples from tight gas sand field	$b = 0.011\ (D/\phi)^{-0.53}$	46
Data in the literature and from industrial sources	$b = 0.0094\ (D/\phi)^{-0.5}$	18

theoretical formulation including tortuosity	$b = \beta(D/\phi)^{-0.5}$	17
theoretical formulation including fractal features	$b = X\ (\beta/\mu)\sqrt{(2/\tau)}(D/\phi)^{-0.5}$	52
theoretical formulation including fractal features	$b = X\ (D/\phi)^{-0.5} + Y\ (D/\phi)(1-(\xi_{max}/\xi_{min})^{1+\lambda-Df})$	47

Table 5: Overview of existing *Klinkenberg* factor correlations.

K_{liq} : liquid *permeability* ; ϕ: porosity; β: correlation coefficient = $\mu(\pi RT/\tau M)^{-0.5}$. τ is the tortuosity, M is the gas molar volume, *T* is the temperature, R is the universal gas constant and μ is the viscosity. $X = (8\mu\ (3+\lambda-D_f)/\ (2+\lambda-D_f)).(32\ \tau(\ 4-D_f/2-D_f)\ (1-\phi)^{-0.5}$ where λ and D_f are the fractal dimensions for tortuosity and for pore space.

$Y = A(8\mu\ (3+\lambda-D_f)/\ (2+\lambda-D_f)).(32\ \tau(\ 4-D_f/(2-D_f)\ )\ (1-\phi)^{-0.5}\ (\pi RT/2M)^{-0.5}$

and $Z = = B(8\mu\ (3+\lambda-D_f)/\ (2+\lambda-D_f)).(32\ \tau(\ 4-D_f/(2-D_f))\ (1-\phi)^{-0.5}\ (\pi RT/2M)$. Based on experimental estimation results, A and B are taken as 1.25 and 0.23, respectively (54)

5. Conclusion

The p*ermeability* of aerogels is a key parameter for many applications and synthesis processes (drying, SCD, doping, impregnation) but surprisingly only a few studies are available in the literature. It is probably difficult to measure the inner flow because of the low *permeability* and mechanical properties of aerogels. The fluid in the pores exerts stress on the network and can result in the fracture of the solid network of aerogels. Consequently, different alternative methods like thermal expansion, the three-point bending technique, and impregnation are proposed depending on the range of *permeability* and the mechanical properties of the gels. The *permeability* values we obtained with these techniques were 1 – 20 nm² for classic silica gels and up to 65 nm^2 for composite aerogels.

The permeability of composite gels was measured with nitrogen and water on the same specimens. Results showed that the gas *permeability* was 20-30 times higher than liquid permeability . The problem of predicting intrinsic *permeability* from gas permeability is based

on the "gas slippage" theory. However, this study shows that it is generally not easy to extrapolate the intrinsic *permeability* of aerogels from gas *permeability* and slippage models because it requires knowledge of a set of porous features like porosity, hydraulic diameter, *Knudsen* number, tortuosity, etc., thus limiting the applicability of these semi-empirical models.

The use of the aerogels not only as an end material but also as a host matrix is an interesting alternative. However, the properties that are required for a silica aerogel as a host matrix are completely different from those usually required, which are a large pore volume and specific surface area, low thermal conductivity or sound velocity and consequently poor mechanical properties. When the aerogel is to be used as a host matrix, the main properties required are high mechanical stability and a large mean pore size (high *permeability*). Different kinds of aerogels to be used for different purposes thus require different research approaches to propose a synthesis process able to achieve these objectives. In practice, a “good host matrix aerogel” is a compromise between the classical aerogel and porous glasses.

Aerogel has specific properties thanks to its very high porosity, filling and/or sintering the porous structure are other ways to exploit the advantages and increase the range of applications of aerogels in the future.

References

1 Woignier T, Reynes J and Phalippou J (2020) Porous Glasses, Binary Glasses and Composite Glasses from Aerogels. Same Issue

2 Woignier T, Phalippou J, and Prassas M (1990) Glasses from aerogels part 2: The aerogel glass transformation. J Mater Sci 25: 3118–3126.

3 Scherer G (1989) Measurement of permeability I. Theory. J Non-Cryst Solids 113: 107 - 118

4 Beurroies I, Bourret D, Sempéré R, Duffours L, Phalippou J (1995) Gas permeability of partially densified aerogels. J Non-Cryst Solids 186, 328 – 333
(16)

8 Scherer G, Hdach H, Phalippou J (1991) Thermal expansion of gels: a novel method for measuring permeability . J. Non-Cryst. Solids. 130: 157 - 170

9 Brinker JF, Scherer GW (1990) Sol-Gel Science, Academic Press, N.Y.

10 Phalippou J, Scherer G, Woignier T, Bourret D, Sempéré R (1995) Ultraporous materials with low permeability . J Non-Cryst. Solids 186: 64-72

11 Scherer GW (1992) Bending of Gel Beams: method of characterizing mechanical properties and permeability . J Non-Cryst Solids 142 [1-2]: 18-35

12 Scherer GW (1994) Hydraulic Radius and Mesh Size of Gels. J Sol-Gel Sci. and Techn. 1:285–291

13 Woignier T, Scherer GW, Allaoui A. (1994) Stress in aerogel during depressurization of autoclave: II. Silica gels. J Sol-Gel Sci Technol 3:141-150

14 Scheidegger AE (1974) The physics of flow through porous media. 3rd edition, University of Toronto Press. Toronto-USA.

15 Swami V (2012) Shale Gas Reservoir Modeling: From Nanopores to Laboratory SPE163065, STU, SPE Annual Technical Conference and Exhibition, 8-10 October, San Antonio, Texas, USA http://dx.doi.org/10.2118/163065-STU

16 Anez L, Calas-Etienne S, Primera J, Woignier T (2014) Gas and liquid permeability in nanocomposite gels : comparison of Knudsen and Klinkenberg correction factors . Microporous and Mesoporous Materials 200 :79-85

17 Civan F (2010) Effective Correlation of Apparent Gas Permeability in Tight Porous Media. Transp Porous Med. 82: 375-384

18 Florence F, Rushing JA, Newsham KE, Blasingame TA (2007) Improved Permeability Prediction Relations for Low Permeability Sands. SPE 107954:1

19 Scherer GW, Hdach H, Phalippou J (1991) Thermal expansion of gels: a novel method for measuring permeability J. Non-Cryst Solids 130:157-170

20) Scherer G (1997) Effect of drying on properties of silica gel. J Non Cryst Solids 215:155-168

21 Scherer G (1994) Relaxation of a viscoelastic gel bar: I. theory. J Sol Gel Sci and Techn. 2:169-175

22 Quinsson JF, Repellin –Lacroix M, Pauthe M , Roche A, Scherer GW(1994) Structure and permeability of gels. J Sol Gel Sci. and Techn. 2 : 239-244

23 Reynes J, Woignier T, Phalippou J (2001) Permeability measurements in composites aerogels: application to nuclear waste storage. J Non-Cryst Solids 285: 323–327

24 Woignier T, Primera J, Lamy M, Fehr C, Anglaret E, Sempere R, Phalippou J (2005) The use of gels as host matrices for chemical species. Different ways to control the permeability and the mechanical properties. J Non-Cryst Solids 350:298-306.

25 Carman P (1937) Flow of gases through granular beds. Trans Inst Chem Engrs.15: 150 -166.

26 Primera J (2002) Synthèse, Structure et Propiétés de Transport des Gels Composites SiO2-SiO2 : Etude expérimental et Simulation. PhD Thesis Université de Montpellier 2, Montpellier France.

27 Katz AJ, Thompson AH (1986) Quantitative prediction of permeability in porous rock. Phys Rev B Condens Matter.198634(11):8179-8181

28 Scherer GW (1994) Effect of drying on viscoelasticity and permeability of gel, in Better Ceramics Through Chemistry VI, eds. A.K. Cheetham, C.J. Brinker, M.L. Mecartney, and C. Sanchez (Mat. Res. Soc., Pittsburgh, PA) pp. 209-215

29 Toki M, Miyashita S, Takeuchi T, Kande S, Kochi A (1988) A large-size silica glass produced by a new sol-gel process. J Non-Cryst Solids 100: 479–482

30 Sanaei A, Jamili A, Callard J (2014) "Effects of non-Darcy flow and pore proximity on gas condensate production from nanopore unconventional resources" in "5th International Conference on Porous Media and Their Applications in Science, Engineering and Industry", Vafai K, Bejan A, Nakayama A, Manca O, Eds, ECI Symposium Series, http://dc.engconfintl.org/porous_media_V/33

31 Gelb LD, Gubbins KE, Radhakrishnan R, Sliwinska-Bartkowiak M (1999) Phase Separation in Confined Systems. Reports on Progress in Physics 62:1573-1659. http://dx.doi.org/10.1088/0034-4885/62/12/201

32 Rahmani Didar B,Akkutlu IY (2013). Pore-size Dependence of Fluid Phase Behavior and Properties in Organic-Rich Shale Reservoirs SPE-164099, SPE Int. Symposium on Oilfield Chemistry held in Woodlands, Texas, USA, 8–10 April. https://doi.org/10.2118/164099-MS

33 Sanaei A, Jamili A, Callard J, and Mathur A (2014) Production Modeling in the Eagle Ford Gas Condensate Window: Integrating New Relationships between Core Permeability , Pore Size, and Confined PVT Properties" SPE-169493.SPE Western North American and Rocky MountainJoint Regional Meeting. Society of Petroleum Engineers. doi:10.2118/169493-MS

34 Devegowda D, Sapmanee K, Civan F, Sigal R (2012) Phase Behavior of Gas Condensates in Shales Due to Pore Proximity Effects: Implications for Transport, Reserves and Well Productivity , SPE Annual Technical Conference and Exhibition, 8-10 October, San Antonio, Texas, USA SPE-160099-MS: http://dx.doi.org/10.2118/160099-MS

35 Jin L, Ma Y, and Jamili A (2013) Investigating the Effect of Pore Proximity on Phase Behavior and Fluid Properties in Shale Formations. SPE Annual Technical Conference and Exhibition, New Orleans, USA, 30 September–2 October. SPE-166192-MS. http://dx.doi.org/10.2118/166192-MS.

36 Wu Y, Pruess K, Persoff P (1998) Gas flow in Porous Media with Klinkenberg Effects. Transp in Por Media. 32, 117 – 137

37 Klinkenberg, L (1941) The permeability of porous media to liquid and gases. API Drilling and Production Practice. 200 - 213

38 Miguel AF, Serrenho A (2007) On the experimental evaluation of permeability in porous media using a gas flow method, J of Physics D: Applied Physics 40 (21): 6824-6828

39 Schaaf SA, Chambre PL (1961) Flow of Rarefied Gases, Princeton University Press,

Princeton, NJ, USA

40 Ziarani AS, Aguilera R (2012) Knudsen's Permeability Correction for Tight Porous Media.Transp Porous Med 91:239-260

41 Jones S, Owens WW (1980) A laboratory study of low permeability gas sands. J Petroleum Technol 32(9):1631-1640

42 Tanikawa W, Shimamoto T. (2009) Comparison of Klinkenberg-corrected gas permeability and water permeability in sedimentary rocks. International Journal of Rock Mechanics & mining Sciences. 46, 229 - 238

43 Heid J, Mc Mahon JJ, Nielson RF, Yuster ST (1950) Study of the permeability of Rocks to homogeneous Fluids in Amer. Pet. Inst. Drilling and Production Practice 230. API Drilling and Production Practice. 230-246

44 Jones S (1972) A rapid accurate unsteady-state Klinkenberg parameter. Society of Petroleum Engineers Journal 12(5):383-397

45 McPhee C, Arthur K (1991) Klinkenberg Permeability measurements: Problems and Practical Solutions. In: Advances in Core Evaluation II. Reservoir Appraisal. Reviewed Proceeding of the second Society of Core Analysts. European Core Analysis Symposium. p. 371. Gordon and Beach Science Publishers, London, UK

46 Sampath CW, Keighin K 1982. Factors affecting gas slippage in tight sandstones. Paper SPE 9872.J. Petrol. Technol, 34: 2715–2720. doi: 10.2118/9872-PA.

47 Song W , Yao J, Li Y, Sun H, Yang Y (2018) Fractal models for gas slippage factor in porous media considering second-order slip and surface adsorption. International Journal of Heat and Mass Transfer 118: 948-960

48 Tang, GH, Tao WQ, He YL (2005) Gas Slippage effect on microscale porous flow using the lattice Boltzmann method. Phys. Rev. E, 72 (056301) doi/10.1103/PhysRevE.72.056301

49 Beskok A, Karniadakis GE (1999) A model for flows in channels, pipes, and ducts at micro and nano scales, Nanoscale Microscale Thermophys Eng 3:43-77

50 Woignier T Primera J T Reynes J (2016) Nanoporous materials for nuclear waste containment . J Nanomaterials (3):1-10, doi 10.1155/2016/4043632

51 Woignier T, Anez L, Calas-Etienne S, Primera J (to be published) Gas slippage in fractal porous materials. Accepted in Journal of Natural Gas Science & Engineering

52 Zheng Q, Yu B , Duan Y, Fang Q (2013) A fractal model for gas slippage factor in porous media in the slip flow regime Chem. Eng. Sc. 87:209-215.

53 Loyalka S, Hamoodi S (1990). Poiseuille Flow of a Rarefied Gas in a Cylindrical Tube: Solution of Linearized Boltzmann Equation. Phys. Fluids A. 2(11): 2061–2065. http://dx.doi.org/10.1063/1.857681.

54 Maurer J, Tabeling P, Joseph P, Willaime (2003) Phys. Fluids 15(9): 2613-2621

https://doi.org/10.1063/1.1599355

55 Kim SH and Pitsch H 2008 Analytical solution Solution for a higher –order Lattice Boltzman Method: slip velocity and Knudsen Layer. Phys.Rev. E , vol. 78, no. l, 016702, https://www.researchgate.net/publication/321221857_

56 Wu L , Bogy DB, 2001 A generalized compressible Reynolds lubrication equation with bounded contact pressurePhys. Fluids, 13:2237–2244

57 Lu YB, Tang GH, Sheng Q, Gu XJ, Emerson DR Zhang YH 2017 Knudsen's permeability correction for gas flow in tight porous media using the R26 moment method. Journal of Porous Media 20(9):787-805 DOI: 10.1615/JPorMedia.v20.i9.20

Thierry Woignier is Director of Research, CNRS (IMBE). He is graduated as engineer in Materials Sciences, PhD in Physics (1984), and State Doctorate in Physics (University Montpellier, 1993). He directed research teams in Montpellier CNRS and since 2006 he directs the Physical Properties of Soils laboratory at The Caribbean AgroEnvironmental Campus (Martinique). He was responsible of Research Programs on aerospace applications, nuclear waste containment, and pesticides remediation.

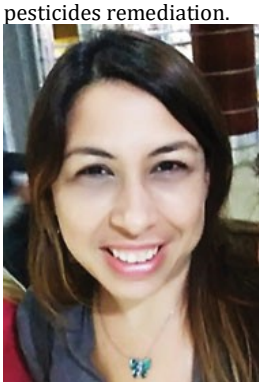

Liz Anez -Borges is a professor at the Physics Department of engineering school at University of Zulia – Venezuela, where she also coordinates the postgraduate studies in Applied Physics. At this university she obtained her Bachelor's degree in Industrial Engineer (2001), Master's degree in Applied Physics (2006), and an Environmental Engineering Doctorate (2010). She also has a Doctorate in Physics (2009) from University of Montpellier. Her research fields are the physical properties of porous media and CO2 sequestration through carbonation reactions.

Sylvie Calas-Etienne is graduated as engineer in Materials Science in 1992, PhD in Physics of Materials in 1997, and State Doctorate (University of Montpellier) in 2012. She is an assistant professor in Charles Coulomb Laboratory (L2C) of University of Montpellier. Her research focuses on ultraporous materials (aerogels) and hybrid organicinorganic coating for surface structuration.

Juan Primera Ferrer is Professor Emeritus in the Physics Department f the University of Zulia. He obtained his Bachelor's degree in Physics om the University of Zulia (Maracaibo) in 1991, and his doctorate at the University of Montpellier, France, in 2002. He is Full Time Principal Professor at the Technical University of Manabí, Ecuador. His research focuses on the transport properties in disordered systems (aerogels).

Pascal Etienne is a professor at the University of Montpellier. He is graduated as engineer in Materials Sciences, obtained a PhD in Physics in 1993, and the accreditation to direct research in 2000. He is managing the research team "Hybrid and nanostructured Materials" from the Charles Coulomb's laboratory and the Platform of OptoMicrofluidic of Montpellier (POMM). He is a specialist of Hybrid Organic-Inorganic materials involved in the sol–gel process and used especially in surface functionalization and microstructuration.

Jean Phalippou was a professor at the University of Montpellier, and has received PhD from the University of Montpellier (France) in 1968. He taught at the "Polytec" engineer school and Montpellier University. He was one of the pioneer scientists who identified the promising future for sol–gel processing and made numerous contributions of great impact to its foundation and development. Professor Phalippou was a reference in the field of the synthesis of glasses from gels and aerogels. He passed away in November 2017.